J Nanostruct 16(4): 5726-5736, Autumn 2026

RESEARCH PAPER

Zinc Nanoparticle Synthesis Using Ginger Extract by Laser Ablation Method: Characterization, Antifungal, Antioxidant Activity, and Hemolytic Toxicity

Abdulsalam M. Hasan [1], *Salma S. Abdullah* [1*], *Sabah A. Salman* [2]

[1] *General Directorate for Education of Diyala, Diyala, Iraq*

[2] *Department of Physics, College of Science, University of Diyala, Diyala, Iraq*

ARTICLE INFO

Article History:
Received 13 July 2026
Accepted 17 September 2026
Published 01 October 2026

Keywords:
Antibacterial activity
Laser ablation
Zinc nanoparticles
Zingiber officinale

ABSTRACT

The pursuit of producing nanoparticles without using toxic chemicals as coating agents has led to the development of pulsed laser ablation. Current research focuses heavily on inorganic nanoparticles due to their low toxicity and high efficacy as antibacterial agents in treating various infectious diseases. Given the resistance of microbial strains, further research on antimicrobial drugs is essential. In this study, zinc nanoparticles (ZnNPs) were produced within extracted ginger liquid using pulsed laser ablation. UV-VIS spectroscopy revealed a peak surface plasmon resonance of the produced zinc nanoparticles over time. Fourier transform infrared spectroscopy was used to evaluate the properties of the functional groups in the active chemicals used in the synthesis of the zinc nanoparticles. The synthesis of the nanoparticles using an environmentally friendly methodology, as well as their antibacterial efficacy, were confirmed. The efficacy of zinc nanoparticles at different concentrations (12.5, 25, 50, 75, and 100 mg/ml) was evaluated against Gram-negative bacteria (*Escherichia coli and Klebsiella pneumoniae*) and Gram-positive bacteria (*Staphylococcus aureus and Streptococcus species*). The antibacterial activity showed a broad inhibition zone at a concentration of 100 mg/ml. Zinc nanoparticles can act as an antibacterial agent in the treatment of diseases caused by harmful microorganisms. This work aims to highlight the antibacterial activity of zinc nanoparticles extracted from ginger root using an environmentally friendly technique.

How to cite this article
M. Hasan A, S. Abdullah S, A. Salman S . Zinc Nanoparticle Synthesis Using Ginger Extract by Laser Ablation Method: Characterization, Antifungal, Antioxidant Activity, and Hemolytic Toxicity. J Nanostruct, 2026; 16(4):5726-5736. DOI: 10.22052/JNS.2026.04.101

INTRODUCTION

The alarming growth of infectious diseases and dangerous microorganisms is a major cause for concern. Compared with their bulk equivalents, particles at the nanoscale exhibit unique physicochemical characteristics. A number of medical uses exist for nanoparticles (NPs), including biosensors, imaging, cancer treatment, drug delivery systems, diagnostic tools, and biosensors [2–4]. NPs possess a high surface-to-volume ratio, endowing them with distinctive features and enhancing their potential

* *Corresponding Author Email: dr.salmaalshamari@gmail.com*

This work is licensed under the Creative Commons Attribution 4.0 International License.
To view a copy of this license, visit http://creativecommons.org/licenses/by/4.0/.

for biomedical applications. NPs are primarily categorized into three categories in biological applications on the basis of their chemical structure [5,6]. And have a bigger surface area available for contact with microorganisms than micro particles Organic (such as polymers and liposomes) and inorganic NPs (such as metals, metal oxides, quantum dots, ceramics, and carbon-based NPs) are encompassed by this phrase [7–9]. Various methodologies for synthesizing metallic NPs include chemical reduction, electrochemical synthesis, hydrothermal methods, electrophoresis, photochemical synthesis, template-assisted synthesis, chemical vapor deposition, sol–gel processes, pyrolysis, and nanoemulsion. The unique physicochemical properties, biocompatibility, and therapeutic potential of Zn NPs have garnered significant interest as novel nanomaterials. The scientific community is highly intrigued by the potential of Zn NPs as a cancer treatment. Several studies have confirmed that these particles are effective against cancer cells [11]. Zn NPs provide numerous advantageous characteristics and distinct benefits compared with other NP kinds in terms of efficacy, selectivity, and the development of medicine resistance. Ginger, the rhizome of *Zingiber officinale*, has been utilized for therapeutic purposes since ancient times. It has been a significant plant in the old pharmacopoeias of China and India. Various constituents of ginger, including 6-gingerol, 6-shogaol, and Galano lactone, have been documented to exhibit anti-5HT3 action [12,13]. *Z. officinale* is utilized to address a range of gastrointestinal issues, including motion sickness, morning sickness, dyspepsia, flatulence, and diarrhea. It is utilized for the management of nausea induced by cancer therapy, postoperative nausea and vomiting, and appetite loss [14–16]. It is also utilized as a digestive aid for mild gastrointestinal disturbances, cough, persistent bronchial issues, low-grade infections of various types, and anorexia situations. *Z. officinale* is presently available in the forms of extract (Zinaxin), tincture (Bioforce Jan De Vries), pill, and oil for oral use. The present study examined the impact of Zn and aqueous ginger extract, produced via pulsed laser ablation mothed, on certain physical attributes and biological activities of specific bacterial strains.

MATERIASL AND METHODS

Synthesis of Zn NPs

A pure zinc plate (purity level of 99.66%), measuring (1 cm × 1 cm × 2 mm), was immersed in 5 mL of deionized distilled water in a beaker 5 cm from the laser source. It was used in the pulsed laser ablation technique in liquid to remove organic contaminants from the target, which had been previously purified using ethanol and distilled water. A Q-switched Nd:YAG laser that pulses 1000 times per wavelength, has an energy output of 500 mJ, and operates at a repetition rate of 1 Hz was used at a wavelength of 1064 nm. First, plant extract was prepared by purifying and rinsing zingiber root leaves with deionized water. Subsequently, the plants were chopped into small pieces, added to a 100 mL beaker together with 80 mL of deionized water, and stirred at 80 °C for 1 h. Filter paper was used for filtering to further purify the extract solution. Fig. 1 shows

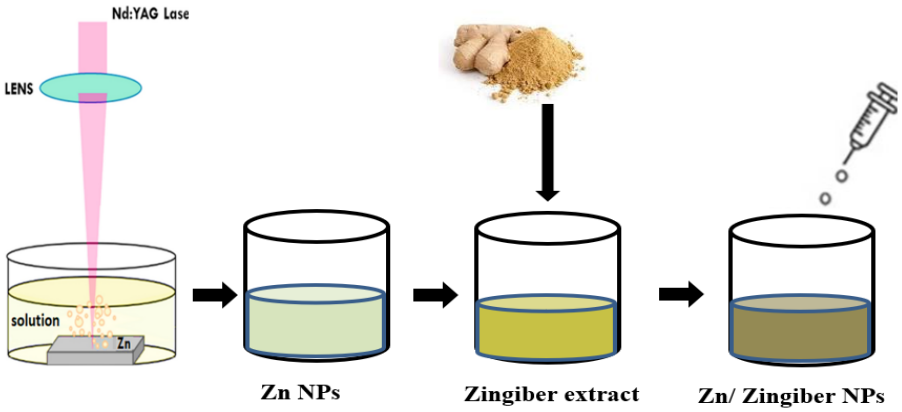


Fig. 1. Schematic of preparation and synthesis of Zinc nanoparticles using pulsed laser ablation and zingiber extract.

CC BY

the overall process for creating ZnNPs via pulsed laser ablation using zingiber extract. ZnNPs were identified, and their synthesis from ginger extracts was verified using absorption spectra and surface plasmon resonance (SPR) obtained using a Shimadzu Double Beam 1800 UV spectrometer from Japan. Nano-solutions were mixed with KBr granules to determine the effective aggregation of NPs synthesized in different solvents, and the infrared spectra were characterized across the wavenumber range of 400–4000 cm−1 by using a Shimadzu IR Affinity-1CE (Fourier transform infrared spectroscopy, FTIR) spectrophotometer from Japan. field emission scanning electron microscope (FESEM) model (ZEISS SIGMAVP/ Germany).

Antibacterial Activity Tests

Staphylococcus aureus, *Streptococcus spp.*, *Escherichia coli*, and *Klebsiella pneumoniae* were grown on blood agar. Biomeriex's calibration solution was used to count the number of bacterial cells (about 1.5×10^8 cells/mL). With a loop, a series of bacterial colonies was moved to create suspended bacteria. These bacteria were then placed into tubes with brain heart infusion broth. The tubes were kept at 37° C for 18–24 h. The suspended bacteria were evaluated against the standard MacFarland solution at a concentration of 1.5×10^8 cells/ml. Afterwards, the suspended bacteria were placed on Mueller–Hinton agar plates with a sterile brush and left to dry for a short period. Holes were made in the culture material with a sterilized cork borer. A micropipette was used to place 100 µL of the medication into each well at the doses of 100, 75, 50, 25, and 12.5 µg/mL. The diameter of the inhibitory zone surrounding each hole was assessed to determine how effectively each concentration worked.

Hemolytic Toxicity by Red Blood Cell (RBC) Fragility Test

The RBC fragility test was used to see how well the chemicals could break down RBCs. Fresh human RBCs were washed three times with isotonic saline (0.9% NaCl) and then resuspended to a 2% hematocrit. An equal amount of erythrocyte suspension was mixed with chemical solutions and kept at 37 °C for 1 h. After centrifugation was performed at 1500 rpm for 10 min, the supernatant's absorbance was measured at 540 nm to determine the amount of hemoglobin released. Distilled water was used to check for complete hemolysis (positive control), and isotonic saline was used as the negative control. The percentage of hemolysis was compared with the controls. Osmotic lysis frees hemoglobin from RBCs, and the amount of this protein in the supernatant is directly related to the number of cells that have been lysed. Photometric measurements at 540 nm were conducted to measure the hemoglobin concentration in the supernatants to show that hemolysis occurred. The absorbance of the supernatant from erythrocytes lysed in distilled water was established as 100% hemolysis. The following equation was used to determine how much hemolysis occurred:

$$\text{Haemolysis } (\%) = \frac{\text{Abs}_{\text{sample}}}{\text{Abs}_{\text{erythrocytes in water}}} \times 100 \quad (1)$$

In vitro hemolytic assay using spectrophotometry is a direct and useful means to measure hemolysis quantitatively. This approach assesses the impact of varying biomolecule concentrations on human RBCs. The evaluation of cytotoxicity by hemolytic activity assays has proven to be an efficient alternative screening tool for fundamental toxicity. The evaluation of erythrocyte hemolytic activity against various substances is rapid, reliable, and cost-effective, hence facilitating a reduction in the use of laboratory animals for in vivo testing and furthering the objectives of minimizing, refining, and replacing animal research. The hemolytic activity on human erythrocytes is determined to assess toxicity profiles for human application. The level of in vitro cytotoxicity associated with hemolytic activity is assessed on the basis of mortality rate: 0%–9% indicates non-toxicity, 10%–49% refers to minor toxicity; 50%–89% denotes toxicity, and 90%–100% reflects high toxicity.

Antioxidant Activity by DPPH Free Radical Scavenging Assay

DPPH radical scavenging experiment was conducted to see how well the chemicals worked as antioxidants. A methanol solution of 0.1 mM DPPH was established. One milliliter of each compound was combined with 1 mL of DPPH solution. The mixtures were kept in the dark at room temperature for 30 min, and the amount of light absorbed at 517 nm was determined. Ascorbic acid served as the positive control.

CC BY

The following formula was used to identify the proportion of radical scavenging activity:

$$\text{Scavenging activity } \% = \frac{\text{sample A control} - \text{A}}{\text{A control}} \times 100 \quad (2)$$

where A control is the absorbance of DPPH solution without sample, and sample A is the absorbance with the compound test.

RESULTS AND DISCUSSION

Many different substances, such as transition metal ions, organic compounds, and biological molecules, can be found using this method [19]. The first sign of nano production was the change in color of Zn colloidal solutions from clear to yellowish-brown, with the color changing depending on how many pulses were used. UV–Vis analysis was performed to obtain a first look at ZnNPs. Fig. 2 shows that the peak absorption range was between 295 and 297 nm when the Nd:YAG laser had a wavelength of 1064 nm and an energy of 500 mJ. The highest absorption showed the SPR of NPs. Fig. 2 shows how the hue of the synthesis

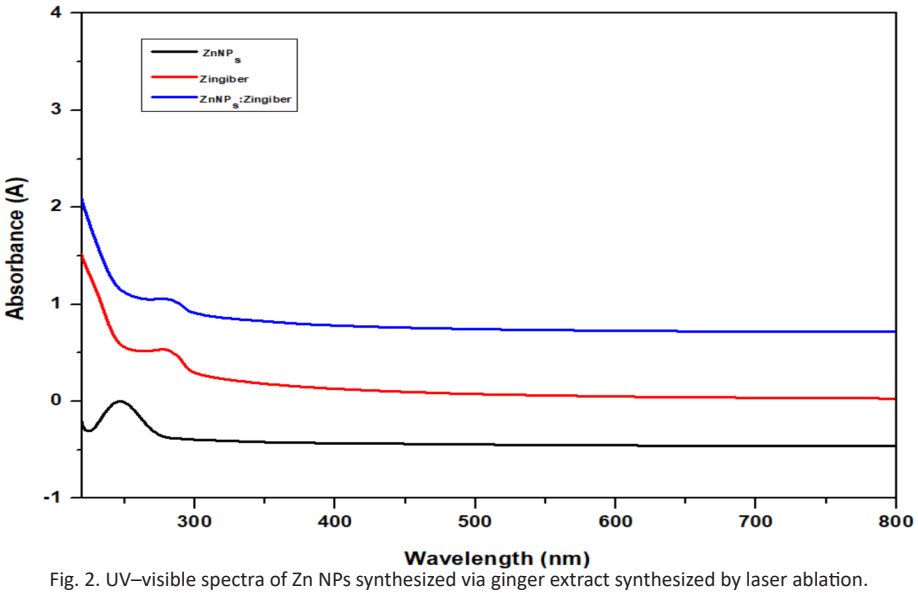


Fig. 2. UV–visible spectra of Zn NPs synthesized via ginger extract synthesized by laser ablation.

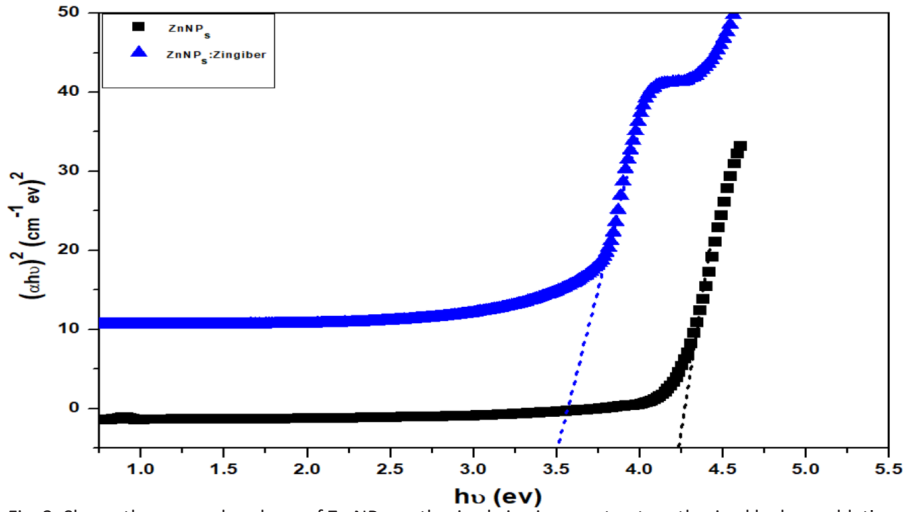


Fig. 3. Shows the energy band gap of Zn NPs synthesized via ginger extract synthesized by laser ablation.

CC BY

solution changed. The Zn combination and the extract solution transitioned from colorless to pale yellow, with the color being constant post-reaction. UV–Vis spectra were acquired relative to water to validate the production of ZnNPs. Fig. 2 illustrates the UV–Vis spectra associated with the ZnNP creation utilizing ginger extracts through pulsed laser ablation. The signal that can be observed in the 400–460 nm region indicated the SPR of the synthesized ZnNPs [20]. The intensity of SPR increased with prolonged reaction time, indicating the production of more ZnNPs. Clusters of ZnNP were continuously generated.

The optical band gap (Eg) of the NPs was ascertained by extrapolating a plot of (αhv) versus the photon energy in the absorption spectra. The absorption coefficient (α) is expressed as $(\alpha hv)^2$, and the intercept provides a dependable estimation of the band gap (Eg) [21]. Fig. 3 demonstrates that the energy band gaps were 4.25 eV for Zn, and 3.5 eV for Zn: Zingiber. The reduction in the band gap correlated with an increase in concentration (the specified eliminator duration), which can be attributed to the quality of the prepared sample. As the eliminator's time increased, the resulting colloid exhibited a more pronounced yellow hue attributed to the ginger extract. The band gap indicates the transfer of electrons from the valence band to the conduction band. A diminished band gap value results in an enhanced transition of electrons to the excited state, hence influencing the adsorption intensity of NPs. The adsorption intensity indicates the transition activity from the excited state to the ground state. The integration of ginger extract into Zn NPs altered the band gap value. The ginger extract can substitute for one of the lattice sites in the Zn crystal structure. Zn has a reduced band gap energy value [22].

The FTIR spectra in Fig. 4 showed absorption peaks that were linked to the vibrations of hydroxyl (O-H), alkane (C-H), aliphatic amines (C-O), and a carboxylic acid (C-O) group. In both pictures, the band below 625 cm^{-1} showed that ZnNPs and their oxides formed. The number of pulses affected the strength of the absorption peaks and the presence or absence of certain peaks because the number of pulses changes the concentration of the solution [23]. The spectra at 3288 and 3275 cm^{-1} were likely due to the ambient moisture during the analysis, and they were related to the OH-stretch bonds of the carboxyl group. The peaks at 1321.2 and 1402.2 cm^{-1} can be attributed to C-O vibrational modes, indicating that CO_2 dissolving in air has no effect [24]. FTIR examination of G-ZnO NPs showed that *Z. officinale* extract works as

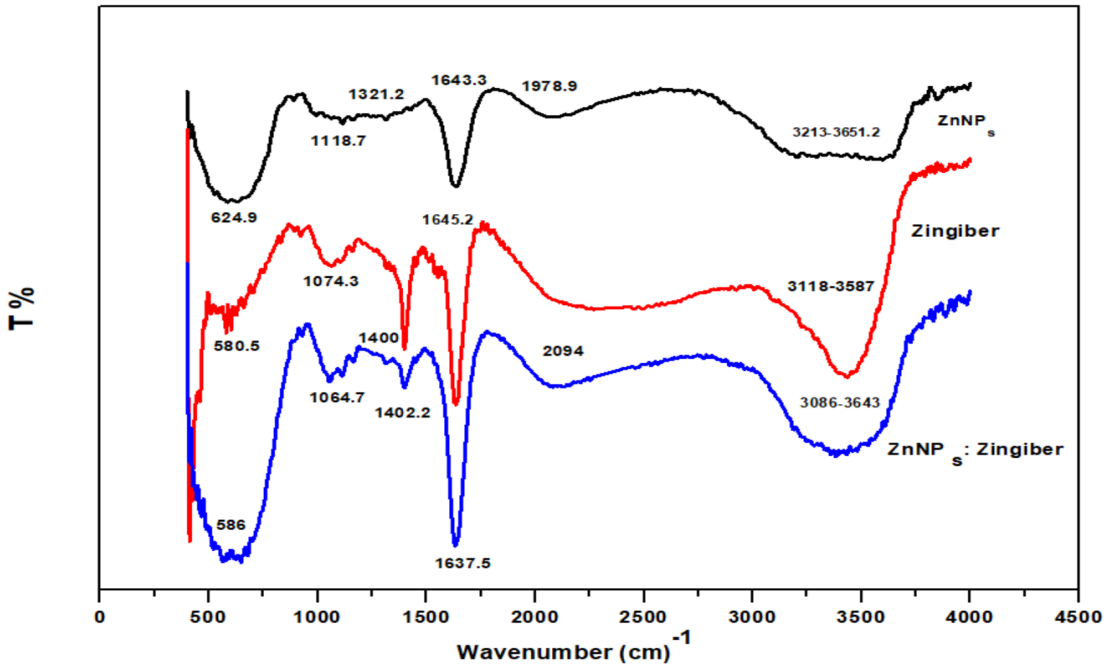


Fig. 4. FTIR spectra of extracts and Zn NPs synthesized laser ablation method.

CC BY

a reducing and capping agent. The broadband coupling at 3439 cm^{-1} showed that the broadband (OH) vibrated in a manner that makes it expand. Peaks were found at 2980, 1579, 1420, 1036, 630, and 465 cm^{-1}, along with their wave numbers and functional groups. Fig. 4 shows organic compounds such as polyphenols, carboxylic and aromatic acids, terpenes, and phenols. The signal at 1579 cm^{-1} clearly showed aromatic compounds, and the peaks at 630 and 465 cm^{-1} showed that G-ZnO NPs were formed by stretching the Zn-O bond. The biological parts of *Z. officinale* are exactly copied

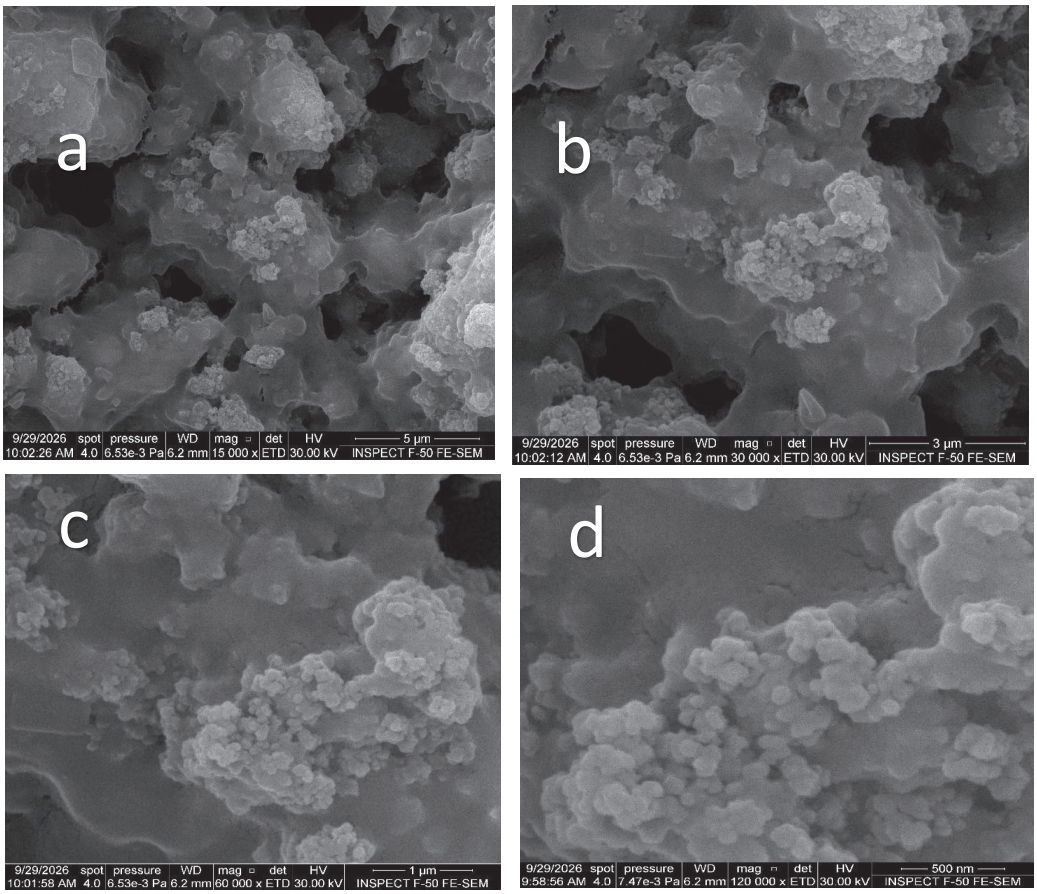


Fig. 5. FESEM images and histogram of extracts and Zn NPs synthesized laser ablation method.

on the surface of NPs [25,26].

Measurement (FE-SEM) of Zn nanoparticles synthesized via ginger extract synthesized by laser ablation was carried out after deposition on quartz as in Fig. 5, where the diameters of the nanoparticles and the standard deviation and largest and smallest diameters of the nanoparticles were recorded. According to scanning electron microscopy (SEM) analysis, the produced zinc oxide nanoparticles (ZnONPs) are spherical and agglomerated, in a previous study, Vidya et al. reported the synthesis of spherical nanoparticles ranging in diameter from 11 to 25 nm [27]. In our study, however, the diameters range from 45 to 78 nm.

Antibacterial Activity

Fig. 6 and Table 1 show how Zn NPs affects *S. aureus*, *Streptococcus spp.*, *E. coli*, and *K. pneumoniae* and Fig. 6 shows Inhibition rate of type of bacteria by using several solutions of Zn NPs. This effect may be attributed to the different sizes and shapes of the Zn NPs made utilizing the green approach. It had an effect on germs, although not as much as its predecessor. The different sizes of NPs, which are very important, alter how they

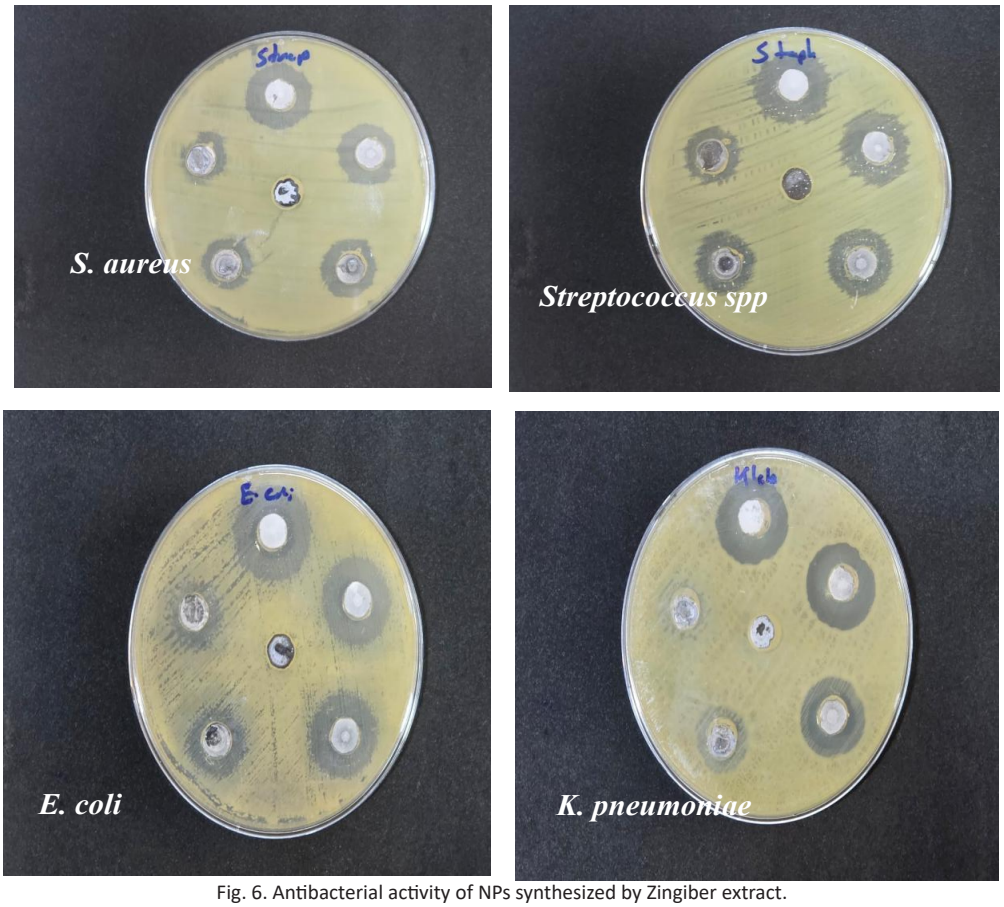


Fig. 6. Antibacterial activity of NPs synthesized by Zingiber extract.

Table 1. Inhibition zone (mm) of type of bacteria at different concentrations of Zn NP_s.

type of bacteria	Concentrations of Zn NP_s.				
	100	75	50	25	12.5
S. aureus	23 mm	20 mm	17 mm	15 mm	14 mm
Streptococcus spp	20 mm	18 mm	16 mm	15 mm	14 mm
E. coli	24 mm	22 mm	20 mm	17 mm	15 mm
K. pneumoniae	22 mm	22 mm	19 mm	17 mm	15 mm

CC BY

affect bacteria. A larger size of NPs makes it easier for them to go through the cell wall and into the nucleus [28]. NPs exhibit increased interaction with bacterial cell membranes, hence augmenting their toxicity in comparison to spherical NPs [29]. NPs effectively target pathogenic bacteria because their surface area is much larger than their volume. Smaller NPs have a larger surface area, which increases their surface charge and accelerates the process of killing or stopping bacteria through electrostatic attraction [28,30]. Fig. 7 shows Inhibition rate of type of bacteria by using several solutions of Zn NPs.

RBC Fragility (Hemolysis) Assay

In the RBC fragility (hemolysis) experiment, the absorbance of the supernatant at around 540 nm quantitatively represents free hemoglobin; thus, a higher absorbance suggests increased membrane damage and RBC lysis. In this work,

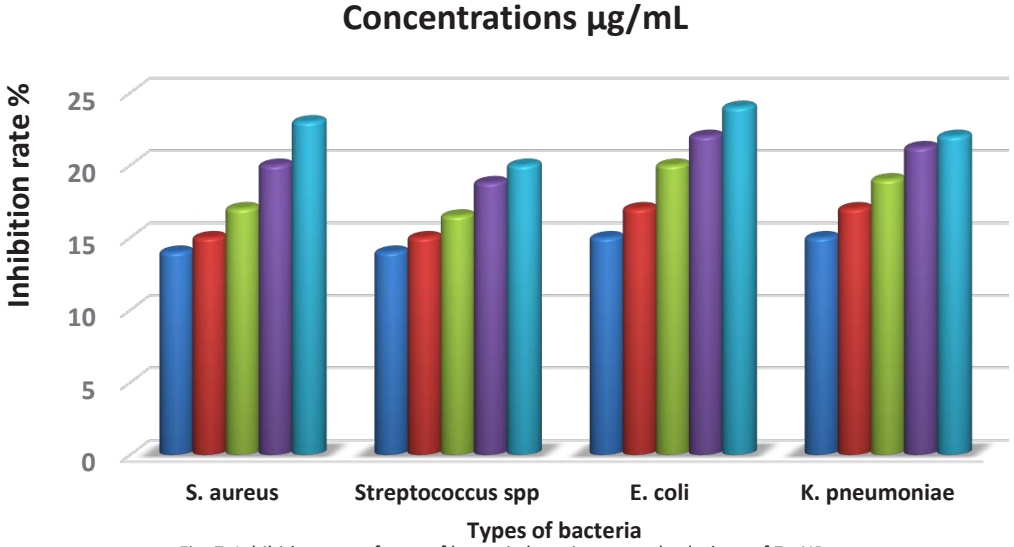


Fig. 7. Inhibition rate of type of bacteria by using several solutions of Zn NP_s.

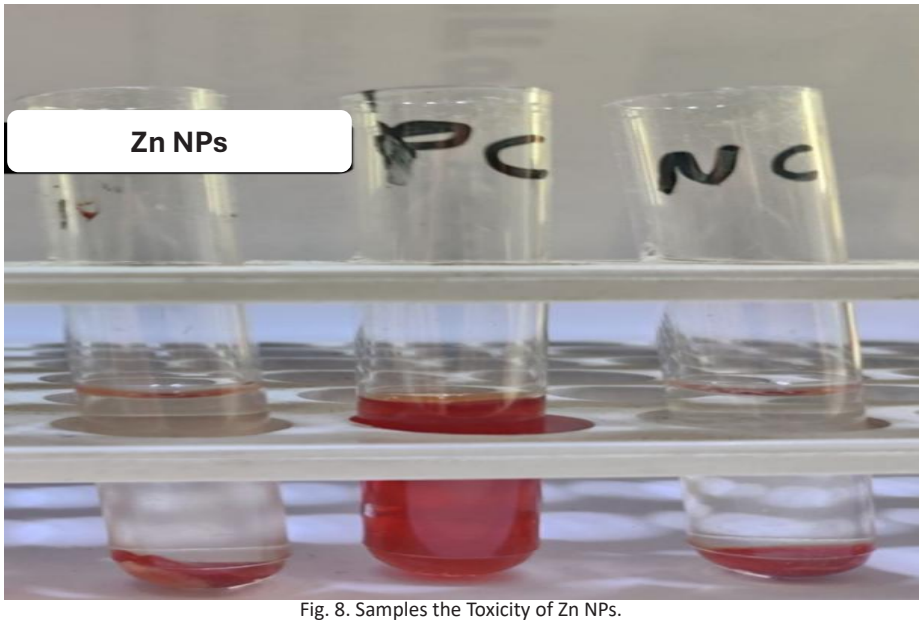


Fig. 8. Samples the Toxicity of Zn NPs.

CC BY

pure water functioned as the positive control (100% hemolysis) and isotonic saline served as the negative control (0% hemolysis) in accordance with recognized protocols for hemolysis assessment [31,32]. A notable detail that different studies and labs use different hemolysis procedures and readout wavelengths, which could make it challenging to compare results. So, the results should be based on the controls and classification system used in the same experiment [33]. Table 2 shows that Zn had a value of 0.019 (1.06%), which is considered non-toxic by the same standards [32]. Fig. 8 illustrates samples the Toxicity of Zn NPs. We observe from the Table 2 all samples were assessed against the same positive control (1.790). DPPH assay measures how well a test sample can lower the purple DPPH radical by measuring how much light it absorbs (usually at ~517 nm). Formula is used to determine the scavengin: I% = [(A_control − A_sample)/A_control] × 100 [34,35]. Your data consistently uses A_control (DPPH) = 1.137, making it easy to compare inhibitory results between samples and concentrations in the same run. Zn had the most significant result, showing a strong suppression at all concentrations (around 93%–95%) and very low absorbance values (0.061–0.079). This finding indicated almost complete DPPH radical quenching, even at 250 µg/mL. Fig. 9 shows samples the Antioxidant assay of Zn NPs.

This Table 3 presents the descriptive statistical analysis of the toxicity assay for tested compounds at a concentration of 1000 µg/ml· For each compound, the number of replicates was three, and the results are expressed as mean absorbance



Fig. 9. Samples the Antioxidant assay of Zn NPs.

Table 2. Value the Toxicity of Zn NPs.

Compound	Concentration µg/ml	Absorbance	Toxicity	Interpretation
Zn	1000 µg/ml	0.019	1.06%	Non-toxic
C+		1.790	100%	Completely toxic
C-		0	0%	Non-toxic

Table 3. Descriptive statistics and multiple-comparison grouping of toxicity absorbance values for the tested compounds at 1000 µg/ml.

Compound	N	Mean absorbance ± SD	Toxicity %	Significance letter
Zn	3	0.019 ± 0.003	1.04	c

CC BY

Table 4. Descriptive statistics and significance grouping of antioxidant activity of the tested compounds at different concentrations.

Compound	Conc. (µg/ml)	N	Mean Abs ± SD	Mean I% ± SD	Significance letter
Zn	250	3	0.086 ± 0.007	92.31 ± 0.62	a
	500	3	0.064 ± 0.013	94.28 ± 1.14	a
	1000	3	0.067 ± 0.006	94.02 ± 0.48	a

Table 5. Value the DPPH assay of Zn NPs.

Concentration	Absorbance	I
1000 µg/ml	0.061	94.64%
500 µg/ml	0.077	93.05%
250 µg/ml	0.079	93.23%
DPPH	1.137	

± standard deviation, together with the calculated toxicity percentage and the post hoc grouping letters. The mean absorbance values showed a clear variation among the tested compound, indicating different toxicity profiles under the same experimental conditions. The lowest absorbance values were recorded for Zn, with mean values of 0.019 ± 0.003, corresponding to toxicity percentages of 1.04%, respectively. compound were assigned to group c, indicating that the difference them was not statistically significant. These findings suggest that Zn had similarly low toxic effects under the applied conditions, despite Zn showing the numerically lowest toxicity among all tested compounds. The grouping letters provide an important statistical interpretation of these differences, where treatments sharing the same letter are not significantly different, while those with different letters differ significantly. Zn was associated with minimal toxicity.

Table 4 and Table 5 summarizes the antioxidant activity of the tested compounds, namely Zn, at three concentrations: 250, 500, and 1000 µg/ml. For each treatment, the results are presented as the mean absorbance ± standard deviation and the mean inhibition percentage (I%) ± standard deviation, based on three replicates. In addition, significance letters are provided to indicate the statistical grouping among treatments, where values sharing the same letter are not significantly different, whereas values with different letters differ significantly. Overall, the results demonstrate clear differences in antioxidant performance among the tested compounds and across the examined concentrations. Among all treatments, Zn consistently exhibited the highest antioxidant activity, with inhibition percentages of 92.31 ± 0.62%, 94.28 ± 1.14%, and 94.02 ± 0.48% at 250.

CONCLUSION

Zinc nanoparticles were effectively synthesized by a cost-efficient, environmentally benign approach of pulsed laser ablation utilising ginger (Zingiber officinale) extract, a process characterized by Fourier transform analysis. The findings indicated that the synthesized zinc nanoparticles demonstrated antibacterial properties. This phenomenon can be ascribed to the reactive oxygen species generated by the nanoparticles in response to bacteria, along with the electrostatic interactions between the nanoparticles and bacterial species. Moreover, the dimensions of the nanoparticles also affected their antibacterial efficacy. The zinc nanoparticles exhibited greater efficacy against Gram-negative bacterial strains than against Gram-positive pathogens. Consequently, employing an eco-friendly technique to synthesize zinc nanoparticles may substantially influence the treatment of disorders induced by harmful bacteria, thereby presenting prospective uses in the pharmaceutical sector.

CONFLICT OF INTEREST

The authors declare that there is no conflict of interests regarding the publication of this manuscript.

REFERENCES

1. Tiki YL, Tolesa LD, Tiwikrama AH, Chala TF. Ginger (Zingiber officinale)-Mediated Green Synthesis of Silver-Doped Tin Oxide Nanoparticles and Evaluation of Its Antimicrobial Activity. ACS Omega. 2024;9(10):11443-11452.

CC BY

2. Faddah H, Nsairat H, Shalan NM, El-Tanani M, Alqudah DA, Alshaer W. Preparation, Optimization and In vitro Evaluation of Doxorubicin-loaded into Hyaluronic Acid Coated Niosomes Against Breast Cancer. Chemistry and Biodiversity. 2024;21(2).
3. Al-Ekaid NM, Al-Samydai A, Al-deeb I, Nsairat H, Khleifat K, Alshaer W. Preparation, Characterization, and Anticancer Activity of PEGylated Nano Liposomal Loaded with Rutin against Human Carcinoma Cells (HT-29). Chemistry and Biodiversity. 2023;20(11).
4. Shakya AK, Al-Sulaibi M, Naik RR, Nsairat H, Suboh S, Abulaila A. Review on PLGA Polymer Based Nanoparticles with Antimicrobial Properties and Their Application in Various Medical Conditions or Infections. Polymers. 2023;15(17):3597.
5. Joudeh N, Linke D. Nanoparticle classification, physicochemical properties, characterization, and applications: a comprehensive review for biologists. Journal of Nanobiotechnology. 2022;20(1).
6. Al Zubaidi ZM, Nsairat H, Shalan NM, Al-Asfoor L, Alqudah DA, Mrahleh M, et al. Hyaluronic Acid – Coated Niosomes for Curcumin Targeted Delivery into Breast Cancer Cells. ChemistrySelect. 2024;9(3).
7. Size Control of Ag Nanoparticles Synthesized by PLA Method in Different Liquid Environments and their Potent against Virulent Candida Albicans. Journal of Pharmaceutical Negative Results. 2022;13(4).
8. Nsairat H, Ibrahim AA, Jaber AM, Abdelghany S, Atwan R, Shalan N, et al. Liposome bilayer stability: emphasis on cholesterol and its alternatives. J Liposome Res. 2023;34(1):178-202.
9. Al-Nasrawi H, Shalan N, Abualsoud BM, Nsairat H. Preparation, characterization and in vitro evaluation of 5-fluorouracil loaded into chitosan–acacia gum nanoparticles. Ther Deliv. 2024;15(5):339-353.
10. Alhaddad R, Abualsoud BM, Al-Deeb I, Nsairat H. Green synthesized Zingiber officinale -ZnO nanoparticles: anticancer efficacy against 3D breast cancer model. Future Science OA. 2024;10(1).
11. Anjum S, Hashim M, Malik SA, Khan M, Lorenzo JM, Abbasi BH, et al. Recent Advances in Zinc Oxide Nanoparticles (ZnO NPs) for Cancer Diagnosis, Target Drug Delivery, and Treatment. Cancers (Basel). 2021;13(18):4570.
12. Sirelkhatim A, Mahmud S, Seeni A, Kaus NHM, Ann LC, Bakhori SKM, et al. Review on Zinc Oxide Nanoparticles: Antibacterial Activity and Toxicity Mechanism. Nano-Micro Letters. 2015;7(3):219-242.
13. Rasmussen JW, Martinez E, Louka P, Wingett DG. Zinc oxide nanoparticles for selective destruction of tumor cells and potential for drug delivery applications. Expert Opinion on Drug Delivery. 2010;7(9):1063-1077.
14. Kebede Urge S, Tiruneh Dibaba S, Belay Gemta A. Green Synthesis Method of ZnO Nanoparticles using Extracts of Zingiber officinale and Garlic Bulb (Allium sativum) and Their Synergetic Effect for Antibacterial Activities. Journal of Nanomaterials. 2023;2023:1-9.
15. Takele E, Feyisa Bogale R, Shumi G, Kenasa G. Green Synthesis, Characterization, and Antibacterial Activity of CuO/ZnO Nanocomposite Using Zingiber officinale Rhizome Extract. Journal of Chemistry. 2023;2023:1-15.
16. Al-Samydai A, Nsairat H, Abu Hajleh MN, Aburas B, Akour A, Ata TeH, et al. Meta-analysis of nano-phytosomes: unleashing the potential of plant-derived compounds for advancing cancer therapy. Nat Prod Res. 2024;39(16):4623-4642.
17. Nsairat H, Jaber AM, Faddah H, Ahmad S. Oleuropein impact on colorectal cancer. Future Science OA. 2024;10(1).
18. Icc ICC, hilo dH, al-garawi zs, ismail hh. Green synthesis of ZnO NPs using ginger extract and assessment of their antioxidant activity. Egyptian Journal of Chemistry. 2022;0(0):0-0.
19. Mohammadi M, Shahisaraee SA, Tavajjohi A, Pournoori N, Muhammadnejad S, Mohammadi SR, et al. Green synthesis of silver nanoparticles using Zingiber officinale and Thymus vulgaris extracts: characterisation, cell cytotoxicity, and its antifungal activity against Candida albicans in comparison to fluconazole. IET Nanobiotechnology. 2019;13(2):114-119.
20. Budhiraja N, Sharma A, Dahiya S, Parmar R, Vidyadharan V. Synthesis and Optical Characteristics of Silver Nanoparticles on Different Substrates. International Letters of Chemistry, Physics and Astronomy. 2013;19:80-88.
21. Julita M, Shiddiq M, Khair M. Determination of Band Gap Energy of ZnO/Au Nanoparticles Resulting in Laser Ablation in Liquid. Indo J Chem Res. 2022;10(2):83-87.
22. Ayuwulanda A, Saputro AH, Permana YN, Saputra IS. Green Dekorasi Au/ZnO Nanokomposit Melalui Media Ekstrak Daun Gaharu (Aquilaria malaccenensis L.) Dan Penentuan Nilai Sun Protection Factor. Jurnal Kimia dan Kemasan. 2021;43(2):126.
23. Stojanovic R, Belscak-Cvitanovic A, Manojlovic V, Komes D, Nedovic V, Bugarski B. Encapsulation of thyme (Thymus serpyllum L.) aqueous extract in calcium alginate beads. Journal of the Science of Food and Agriculture. 2011;92(3):685-696.
24. Nandiyanto ABD, Oktiani R, Ragadhita R. How to Read and Interpret FTIR Spectroscope of Organic Material. Indonesian Journal of Science and Technology. 2019;4(1):97.
25. Birdi T, Daswani P, Brijesh S, Tetali P. In vitro antigiardial and antirotaviral activity of Psidium guajava L. leaves. Indian J Pharmacol. 2011;43(5):616.
26. Khashan KS, Sulaiman GM, Hussain SA. Synthesis and Characterization of Aluminum Doped Zinc Oxide Nanostructures by Nd:YAG Laser in Liquid. Iraqi Journal of Science. 2020:2590-2598.
27. Alqahtani OS, Muddapur UM, Kamat K, Shenvi A, Shaikh IA, Aljaezi I, et al. Sustainable green synthesis of zinc oxide nanoparticles utilizing Zingiber officinale peel aqueous extract, characterization, and determination of its anticancer and antimicrobial potential. PLoS One. 2025;20(11):e0334685.
28. Tuama MJ, Alias MFA. Ecofriendly Synthesis of ZnO Nanoparticles using Zingiber Officinale and Syzygium Aromaticum Extracts for Antibacterial Applications. Iraqi Journal of Science. 2024:4772-4787.
29. Happy A, Soumya M, Venkat Kumar S, Rajeshkumar S. Mechanistic study on antibacterial action of zinc oxide nanoparticles synthesized using green route. Chemico-Biological Interactions. 2018;286:60-70.
30. Alias MFA, Abd – Alsada AS. The Influence of Zinc Oxide with Carbon Nanotube Composite NanoMaterials on Antibacterial Activity. Journal of Physics: Conference Series. 2021;2114(1):012089.
31. Dobrovolskaia MA, Clogston JD, Neun BW, Hall JB, Patri AK, McNeil SE. Method for Analysis of Nanoparticle Hemolytic Properties in Vitro. Nano Lett. 2008;8(8):2180-2187.
32. Pagano M, Faggio C. The use of erythrocyte fragility to assess xenobiotic cytotoxicity. Cell Biochemistry and Function. 2015;33(6):351-355.
33. Sæbø I, Bjørås M, Franzyk H, Helgesen E, Booth J. Optimization of the Hemolysis Assay for the Assessment of Cytotoxicity. Int J Mol Sci. 2023;24(3):2914.
34. Gulcin İ, Alwasel SH. DPPH Radical Scavenging Assay. Processes. 2023;11(8):2248.
35. Baliyan S, Mukherjee R, Priyadarshini A, Vibhuti A, Gupta A, Pandey RP, et al. Determination of Antioxidants by DPPH Radical Scavenging Activity and Quantitative Phytochemical Analysis of Ficus religiosa. Molecules. 2022;27(4):1326.

CC BY